

Magnetic properties of quantum dots and rings

M. Manninen^{1,a}, M. Koskinen¹, S.M. Reimann², and B. Mottelson³¹ Department of Physics, University of Jyväskylä, P.O. Box 35, FIN-40351 Jyväskylä, Finland² Department of Mathematical Physics, Lund University, P.O. Box 118, SE-22100 Lund, Sweden³ NORDITA, Blegdamsvej 17, DK-2100 Copenhagen, Denmark

Received 5 December 2000

Abstract. Exact many-body methods as well as current-spin-density functional theory are used to study the magnetism and electron localization in two-dimensional quantum dots and quasi-one-dimensional quantum rings. Predictions of broken-symmetry solutions within the density functional model are confirmed by exact configuration interaction (CI) calculations: In a quantum ring the electrons localize to form an antiferromagnetic chain which can be described with a simple model Hamiltonian. In a quantum dot the magnetic field localizes the electrons as predicted with the density functional approach.

PACS. 73.21.La Quantum dots – 73.43.Nq Quantum phase transitions – 85.35.Be Quantum well devices (quantum dots, quantum wires, etc.)

1 Introduction

The electronic structure of quantum dots has been an extensive area of research during the last decades [1]. The simple harmonic confinement modeling a quantum dot makes the system especially well suited for applying shell model techniques: The center of mass motion exactly separates out and, on the other hand, a harmonic oscillator basis is a natural starting point [2] for many-body calculations.

When the local spin density approximation has been used to study Hund's rule and the magnetic structure of quantum dots [3], it has been observed that broken symmetry solutions can result. Static spin-density waves of the ground states [3] and the localization caused by a strong magnetic field [4] have, however, been disputed [5,6] as being artifacts of mean field theory since the circular symmetry of the exact Hamiltonian was broken.

In this paper we will first study the spin-density wave in a six electron quantum ring and show that the result of an exact many-body calculation can be mapped to a model Hamiltonian consisting of an antiferromagnetic Heisenberg Hamiltonian, combined with rigid rotations and vibrations. This result confirms the existence of the spin-density wave observed earlier using the local spin density approximation [3,8]. We then study Hund's rule and electron localization of a four electron quantum dot as a function of the electron density. Finally, we will compare the results of exact calculations for six electron dots in magnetic field with those obtained with the current-spin-density formalism, as it originally was developed by

Vignale and Rasolt [7]. For a non-circular dot, we are able to observe the localization caused by a strong magnetic field also in the exact electron density.

2 The model

The electrons are restricted to move in a plane and confined by an external potential (in atomic units)

$$V(r) = \frac{1}{2}\omega_0(r - r_0)^2, \quad (1)$$

where ω_0 is the strength of the confinement and r_0 the radius of the quantum ring ($r_0 = 0$ for a quantum dot). The electrons interact with each other with the normal $1/r$ Coulomb interaction. The many-body Hamiltonian is diagonalized using a configuration-interaction (CI) technique. The spatial single-particle states of the Fock space are chosen to be eigenstates of the single particle part of the Hamiltonian. We expand them in the harmonic oscillator basis. From 30 to about 50 lowest energy single-particle states are selected to span the Fock space. To set up the Fock states for diagonalization, we sample over the full space with a fixed number of spin down and spin up electrons. Only those states with a given total orbital angular momentum and configuration energy (corresponding to the sum of occupied single-particle energies) less than a specific cut-off energy are selected. The purpose was to choose only the most important Fock states from the full basis and hereby reducing the matrix dimension to a size $< 2 \times 10^5$. In the case of a deformed quantum dot in a magnetic field the restriction of the orbital angular momentum could of course not be used.

^a e-mail: manninen@phys.jyu.fi

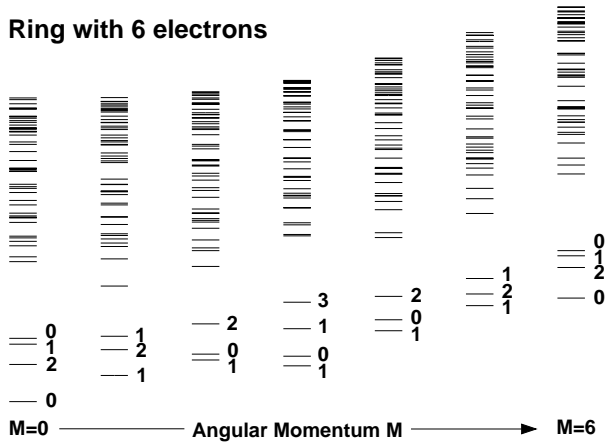


Fig. 1. Many-body spectra of a quantum ring with $N = 6$ electrons ($r_{s,1D} = 2$ a.u. and $C_F = 4$). The energy difference between the yrast states for $L = 0$ and $L = 6$ is 0.143 a.u. The spin S is given for the low-lying states.

The Coulomb integrals between the single particle states were calculated with a numerical integration in a lattice with an accuracy better than 1%. The Hamiltonian matrix was diagonalized with the Arpack library [11] suitable for large sparse matrices.

3 Quantum ring with six electrons

Figure 1 shows the many-body energy spectrum of a quantum ring with six electrons for the potential of Eq. (1) with parameters $\omega_0 = 0.308$ a.u. and $r_0 = 3.82$ a.u. (we use atomic units a.u. for simplicity). These parameters correspond to a one-dimensional density parameter $r_{s,1D} = 2$ a.u. which describes the particle density $n_r = 1/(2r_{s,1D})$ along the ring, and $C_F = 4$, a dimensionless parameter that measures the degree of one-dimensionality. C_F essentially describes the excitation energy of the next radial mode $\hbar\omega_0$, which is defined to be C_F times the (1D) Fermi energy. We thus obtain $\hbar\omega_0 = C_F \hbar^2 \pi^2 / (32m^* r_{s,1D}^2)$. The higher the value of C_F , the more the radial modes are frozen in their ground states. Thus, the ring is narrower for larger C_F (see also Ref. [12].) It is clear from the figure that a band of energy levels separates out from higher energy levels. This band has a six-fold periodicity in the orbital angular momentum M . The lowest levels at $M = 0$, $M = 1$, and $M = 2$ have the same total spin and level spacing as the levels corresponding to $M = 6$, $M = 5$, and $M = 4$, respectively. This band of lowest states for a given angular momentum (which is also called the “yrast” band after the Swedish word for the “most dizzy”) can be understood with a simple model Hamiltonian describing localized spins in a rotating and vibrating “molecule”:

$$H = J \sum_{i,j} \mathbf{S}_i \cdot \mathbf{S}_j + \frac{1}{2I} M^2 + \sum_a \hbar\omega_a n_a, \quad (2)$$

where the first term is an antiferromagnetic Heisenberg Hamiltonian of localized electrons with nearest neighbor

coupling J , the second term describes rigid rotations of a ring of electrons with a moment of inertia I , and the last term describes the vibrational modes of the localized electrons. In Fig. 1 the band gap is that between the lowest and the first excited vibrational state. The spin-structure of the lowest vibrational band is identical to that obtained by diagonalization of the Heisenberg Hamiltonian. (Group-theoretical methods were used to assign the spin-configuration to the orbital angular momentum so that the total wave function has the right symmetry [12]).

In the case of a narrower ring, also the higher vibrational states will separate to individual bands and the energy differences between the different vibrational bands agree well to those calculated from the classical model of six vibrating electrons in a potential of the form of Eq. (1) [12].

4 Quantum dot with four electrons

The rotational spectrum gives a clear signature of localization of electrons in the case of a quantum ring. We examined if the same is true also in the case of a quantum dot, as it was recently conjectured [13,14]. For a six-electron quantum dot, it was found earlier that at $r_{s,2D} = 4$ a.u., the many-body ground state has total spin $S = 0$ and shows antiferromagnetic order in the pair correlation. The polarized state and the state with $S = 1$, both having C_{5v} symmetry and being candidates for the classical ground state configuration [15,16] with five particles localized around one particle in the dot center, were clearly higher in energy [17]. The situation is different, however, for $N < 5$. Here, we discuss a dot and ring confining four electrons, where the classical Wigner molecule only has one stable configuration, a square of electrons. Note that already in the case of six electrons there are two stable classical Wigner molecules, which will make the analysis of the quantum mechanical excitation spectra much more complicated. Figure 2 shows the excitation spectra of a quantum dot with four electrons and, for comparison, those of a ring with four electrons. It is seen that the spectra are qualitatively very similar. In the case of the ring the spectrum can again nearly exactly be described with the Hamiltonian (2), and it has a period of four as a function of the angular momentum (due to the 4-fold symmetry of the square). In the case of the dot, the only qualitative difference is that at $M = 4$ the spin of the two lowest states is the opposite than for $M = 0$. Nevertheless, the similarity of the spectra suggest that with this density of $r_{s,2D} = 4$ a.u. the four electrons in the dot are already nearly localized. The difference of the ring and dot spectra is a result of different vibrational states. Radial oscillations are allowed in the dot, but forbidden in the ring.

Figure 2 also shows that the ground state in both cases has a total spin $S = 1$ according to the Hund’s first rule, and in agreement with the results of the local density approximation [3]. The dependence of the lowest excitation energies with $M = 0$ on the electron density ($r_{s,2D}$) in the dot is shown in Fig. 3. The relative differences between

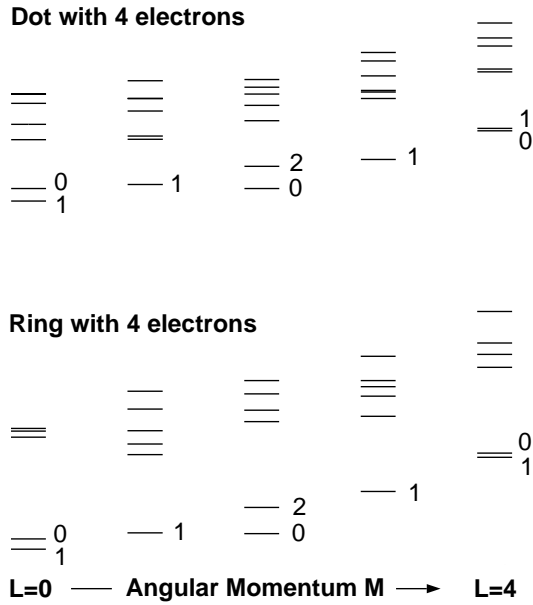


Fig. 2. Rotational spectra (low-lying states) for a quantum dot confining 4 electrons ($r_{s,2D} = 4a_B^*$) (*upper panel*) and a ring ($r_{s,1D} = 2a_B^*$ and $C_F = 10$), each confining four electrons. The energies are rescaled for comparison; the energy difference between the yrast states for $L = 0$ and $L = 4$ is for the dot 0.069 a.u. and for the ring 0.287 a.u., respectively.

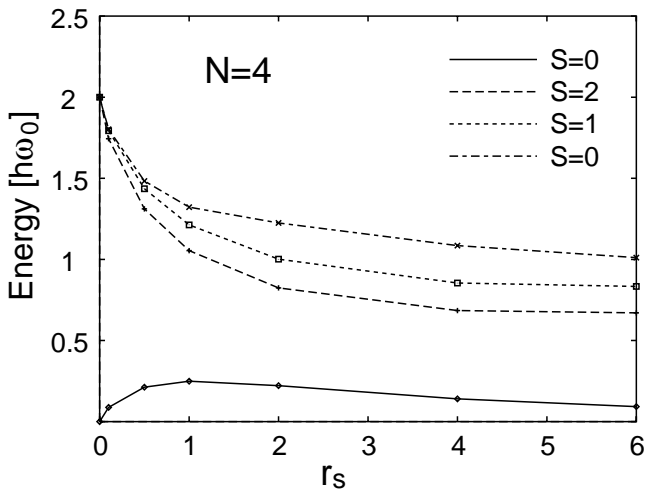


Fig. 3. Lowest excited $M = 0$ states as a function of the electron density parameter $r_{s,2D}$ for a quantum dot with four electrons. The ground state has spin $S = 1$ and the excited states shown in the plot have spin values $S = 0, 2, 1, 0$ (with increasing energy). The energies are given in units of the density-dependent shell $\hbar\omega_0$ ($\omega_0^2 = 1/r_{s,2D}^3 N^{1/2}$).

the energy levels stay the same when the density parameter has reached a value of about $r_{s,2D} = 2$ a.u. indicating that the electron localization in this small system start at a quite high electron density. The ground state remains to be the $S = 1$ state at least up to $r_{s,2D} = 6$ a.u. It should be noted that at large r_s values ($r_{s,2D} = 3$ a.u.) the $M = 1$, $S = 0$ state will be essentially degenerate with the lowest

excited $M = 0$ state shown in Fig. 3. The observation of the Hund's rule ($S = 1$) for the four electron dot seems to contradict CI calculations with much smaller basis [9], but is in agreement with a recent quantum Monte Carlo calculation [10].

5 Localization of electrons in a strong magnetic field

In a strong magnetic field the electron gas in the quantum dot can polarize and form a so-called maximum density droplet (MDD) [18]. The current-spin-density functional formalism [4] and the Hartree-Fock approximation [19] predict that when the magnetic field is further increased, the electrons start to localize and localization begins at the edge of the dot. (However, this localization process in principle is of different character than the formation of Wigner molecules discussed above.)

An exact many-body solution will, also in this case, naturally result in a circularly symmetric electron density and not show this internal localization. The above method of studying the excitation spectrum could also be used in this case to demonstrate the localization. In this study we have, however, chosen another way. We break the symmetry of the Hamiltonian and study deformed, *i.e.* ellipsoidal, quantum dots with six electrons in a strong magnetic field. The exact many-body problem is again solved using the CI technique, which in this case is much more demanding since the orbital angular momentum no longer is a good quantum number. Consequently, the convergence checks show that numerical accuracy of the results is not as good as for the results shown earlier. Nevertheless, we are convinced that the qualitative features of the electron density do not change if the accuracy is increased.

Figure 4 shows the electron densities of circular dots, and Figure 5 the densities of deformed quantum dots confining six electrons, both computed by using the CI method. A comparison to the results obtained in CSDFT confirmed that the maximum density droplet with nearly constant density is obtained at about the same values of the magnetic field both in the CI and CSDFT formalism. When the magnetic field is increased beyond stability of the MDD, the density functional method gives a result showing six maxima corresponding to quasi-localized electrons. The total density of the CI method can show the localization only in the case of the deformed dot. In this case the density is indeed very similar to the result of the CSDFT.

For the circular dot the CI method naturally gives a symmetric solution, while the CSDFT, as a mean field theory, shows the internal symmetry of the state. It should be noted that in the case of the circular dot the ground state of the CSDFT corresponds to the first excited state of the exact calculation, which has one electron in the center of the dot surrounded by a ring of five electrons. The ground state of the CI result corresponds to a single ring of six electrons. Classically, six electrons localized in a circular quantum dot have these two stable configurations with a very small energy difference.

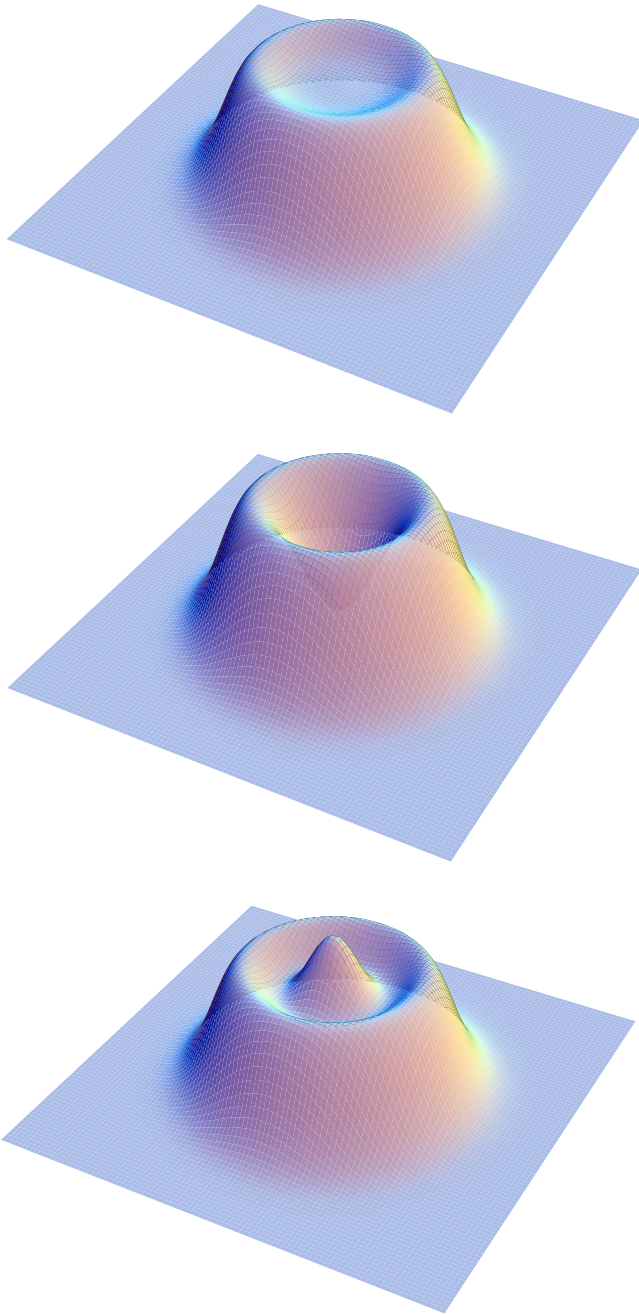


Fig. 4. Electron densities in circular quantum dots confining six electrons. In the *upper panel*, the magnetic field is $B = 0.9$ a.u. and the state is a maximum density droplet. In the *middle and lower panel*, $B = 1.2$ a.u.

6 Conclusions

We showed that the best way to obtain information of internal electron localization in quantum dots and rings is to study the rotational excitation spectrum. When mapped on a model Hamiltonian of an antiferromagnetic Heisenberg lattice of electrons (with rigid rotations and vibrations), the internal structure of the many-body spectrum close to the yrast line can be understood.

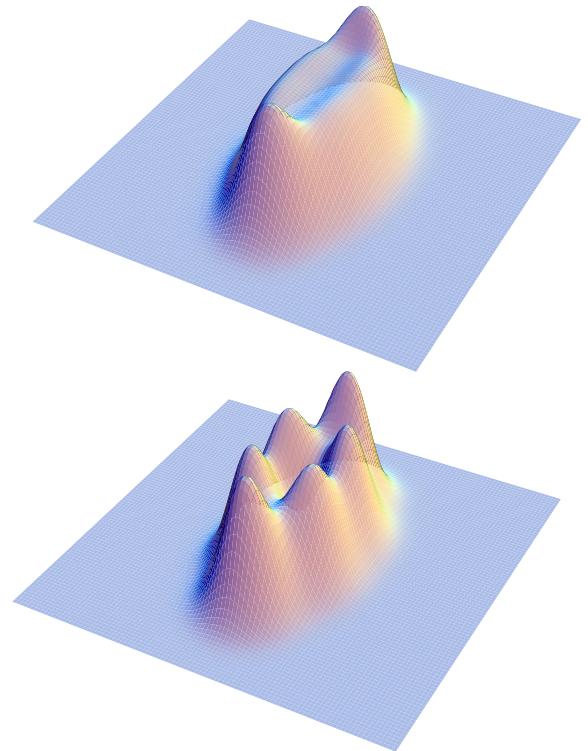


Fig. 5. Electron densities ellipsoidally deformed dots confining six electrons. The magnetic field is $B = 0.9$ a.u. in the *upper panel* and $B = 1.2$ a.u. in the *lower panel*.

In the case of quantum dots the study of the excitation spectrum is more complicated due to the low energy vibrational modes of the localized electrons. When the electron number increases, also the possibility of several local minima of the classical Wigner molecule makes the quantum mechanical excitation spectrum more complicated. Nevertheless, our results indicate that in the case of a four-electron dot the electrons start to localize at quite high electron densities, already when $r_{s,2D} \approx 3$ a.u.

Localization of electrons in a strong magnetic field is demonstrated by breaking the circular symmetry of the quantum dot. In an ellipsoidal quantum dot the exact electron density of six electrons shows clear localization of electrons in agreement with the results of more approximate methods like Hartree-Fock and current-density functional theory.

This work has been supported by the Academy of Finland under the Finnish Centre of Excellence Programme 2000-2005 (Project No. 44875, Nuclear and Condensed Matter Programme at JYFL). S.M.R. thanks the “Bayerische Staatsministerium für Wissenschaft, Forschung und Kunst” for support.

References

1. P. Harrison, *Quantum wells, wires and dots* (Wiley, New York, 1999).
2. T. Chakraborty, *Quantum dots: a survey of the properties of artificial atoms* (Elsevier, Amsterdam, 1999).

3. M. Koskinen, S.M. Reimann, M. Manninen, Phys. Rev. Lett. **79**, 1389 (1997).
4. S.M. Reimann, M. Koskinen, B. Mottelson, M. Manninen, Phys. Rev. Lett. **83**, 3270 (1999).
5. K. Hirose, N. Wingreen, Phys. Rev. B **59**, 4604 (1999).
6. F. Pederiva, C.J. Umrigar, E. Lipparini, Phys. Rev. B **62**, 8120 (2000).
7. G. Vignale, M. Rasolt, Phys. Rev. B **37**, 10685 (1988).
8. S.M. Reimann, M. Koskinen, M. Manninen, Phys. Rev. B **59**, 1613 (1999).
9. B. Chengguang, R. Wenying, L. Yuoyang, Phys. Rev. B. **53**, 10820 (1996).
10. A. Harju, V.A. Sverdlov, R.M. Nieminen, V. Halonen, Phys. Rev. B. **59**, 5622 (1999).
11. R.B. Lehoucq, D.C. Sørensen, Y. Yang, <http://www.caam.rice.edu/software/ARPACK>.
12. M. Koskinen, M. Manninen, R.B. Mottelson, S.M. Reimann, Phys. Rev. B **63**, 205323 (2001).
13. R. Egger, W. Häusler, C.H. Mak, H. Grabert, Phys. Rev. Lett. **82**, 3320 (1999).
14. C. Yannouleas, U. Landman, Phys. Rev. Lett. **82**, 5325 (1999).
15. F. Bolton, U. Rössler, Superlatt. Microstr. **13**, 139 (1992).
16. V.M. Bedanov, F.M. Peeters, Phys. Rev. B **49**, 2667 (1994).
17. S.M. Reimann, M. Koskinen, M. Manninen, Phys. Rev. B **62**, 8108 (2000).
18. A.H. McDonald, S.R.E. Yang, M.D. Jonson, Aust. J. Phys. **46**, 345 (1993).
19. H.-M. Müller, S.E. Koonin, Phys. Rev. B **54**, 14532 (1996).
20. M. Koskinen, J. Kolehmainen, S.M. Reimann, J. Toivanen, M. Manninen, Eur. Phys. J. **9**, 487 (1999).